Utilizing Photogrammetry and Strain Gage Measurement to Characterize Pressurization of Inflatable Modules

Anil Mohammed

JOHNSON SPACE CENTER

Major: Aerospace Engineering

USRP Spring Session

Date: 29 Apr 2011

Utilizing Photogrammetry and Strain Gage Measurement to Characterize Pressurization of Inflatable Modules

Anil Mohammed[1]
University of Illinois, Urbana-Champaign, IL, 61801

I. Abstract

This paper focuses on integrating a large hatch penetration into inflatable modules of various constructions. This paper also compares load predictions with test measurements. The strain was measured by utilizing photogrammetric methods and strain gages mounted to select clevises that interface with the structural webbings. Bench testing showed good correlation between strain data collected from an extensometer and photogrammetric measurements, even when the material transitioned from the low load to high load strain region of the curve. The full-scale torus design module showed mixed results as well in the lower load and high strain regions. After thorough analysis of photogrammetric measurements, strain gage measurements, and predicted load, the photogrammetric measurements seem to be off by a factor of two.

II. Introduction

In space technologies, there has been a huge push for inflatable structures due to its potential mass and volume savings. Soft-good structures are already being used in space suits, micro-meteoroid and orbital debris protective systems, thermal protection, etc. For deep space exploration space program, possible habitats are being considered which puts inflatable structures under the spotlight for its small packaging size and large volume upon inflation. Understanding a variety of design, analysis, test, and manufacturing methods and how these techniques interact is an important part of effectively and efficiently utilizing soft-goods for desired space and terrestrial applications.

NASA proceeded with this study and integrated a large hatch/frame penetration into an inflatable module designs. These hatch/frame penetrations may be required if multiple ports are needed to attach different modules together.

The test article is constructed as a large torus, referred to as the Phase II article (Fig. 1).

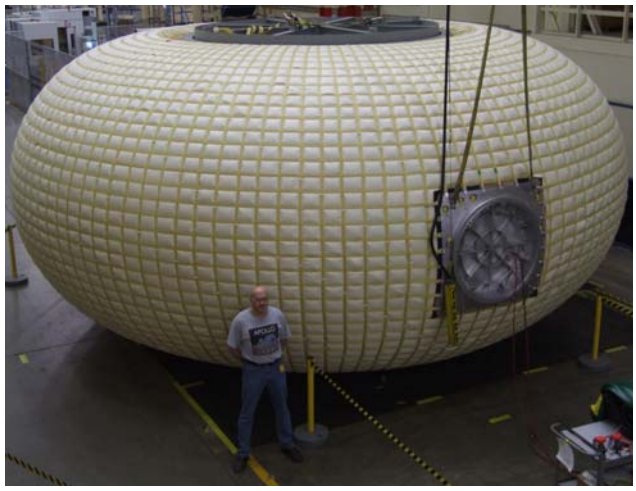

Figure 1. Full-Scale Torus Inflatable Module with Cargo Net Construction

[1] Student, JSC Intern, ES2, University of Illinois at Urbana-Champaign

From a structural standpoint a torus has a geometrical advantage over a large cylindrical structure in that the maximum stress is based on the (smaller) cross-sectional diameter of the torus rather than the (large) diameter of a similarly sized cylindrical structure. These inherently lower stresses allow alternate, lighter weight, restraint layer constructions to be considered. For the Phase II article, the stress is based on the 12.3-foot diameter toroidal cross-section resulting in a relatively lower membrane stress. Therefore, high strength webbing may be spaced further apart, similar to a cargo net type construction, to carry the global pressure loading. A structural bladder (urethane coated Vectran) is used to support the load between structural webbings. For a flight design separate carrier fabric and bladder layers will probably be required to meet leak rate requirements at pressurization. The structural bladder was designed, analyzed and fabricated by ILC Dover for NASA. The restraint layer webbing was designed and analyzed at NASA/JSC and fabricated at ILC Dover. The metallic central core design and fabrication and overall Inflatable Module assembly were completed at NASA/JSC.

The Phase II Inflatable Module assembly was originally designed to support a deployment and mating test in support of a Lunar Surface Systems (LSS) outpost. New direction outlined in the 2011 President's proposed budget included a focus away from near-term (2020) return to the lunar surface and an increased interest in technology development. Therefore, the focus of this project shifted towards a design limit pressurization test.

Most of the man-rated soft good structures use a Factor of Safety of 4.0 for design load. The reasons for this high factor are, uncertainty in manufacturing techniques, difficulty in predicting load path and frictional effects, and limited ability to accurately measure load during testing and accurately correlate it with analytical predictions. When measuring loads in fabric members many measurement devices can be inaccurate or adversely affect the geometry of the soft-good member that is being investigated. In the past, NASA has applied strain gages to metallic clevises that interface with structural webbings to measure strain and thus calibrated load during pressurization with mixed results. For this study, NASA utilized photogrammetry in addition to strain measurement of calibrated clevises to measure strain and load during pressurization. Photogrammetry has been utilized successfully on testing of Composite Overwrap Pressure Vessels (COPV) at WSTF and NASA hopes to demonstrate similar results on a soft-goods structure which are much more flexible when compared to COPV (Reference 1). NASA will use the ARAMIS software system for photogrammetry.

III. Photogrammetry

The Digital Image Correlation system used in this test program was developed by GOM mbH of Braunschweig, Germany and utilizes a software package called ARAMIS. The ARAMIS software uses the principles of photogrammetry that allows full-field displacement and strain measurements. The system requires spraying high contrast dot patterns onto a sample, which is then tracked in ARAMIS by thousands of correlation areas known as facets. The center of each facet is the measurement point that can be thought of as a 3D digital extensometer. An array of these extensometers forms an in-plane strain rosette. The facet centers are tracked in each successive pair of images, with accuracy up to one hundredth of a pixel.

Figure 2 shows an approximate 0.26 inch dot pattern used on the 28 feet diameter vessel. The dot size was chosen to meet a general criteria that each dot occupies 3 to 5 pixels on the camera sensor. Figure 3 shows two 5 megapixel video cameras that were used in the test with a 6 feet camera bar non-standard with the ARAMIS system, and fabricated for the purpose of this test.

The digital cameras were used at a resolution of 2448 x 2050 pixels and recording every 5 seconds, but capable of recording up to 15 frames per second. The ARAMIS cameras work as a stereo pair to create a 3D volume of the area in which the ARAMIS software can take measurements. This volume varies with the angle of the cameras and lens choice. Our camera setup consisted of 12mm lenses with the cameras angled at 24.7 degrees, giving a measuring volume of 2626.3 mm / 2306.8 mm / 2306.8 mm. To calibrate for this volume a 1200-mm calibration object type cross was moved in specified locations to calibrate the sensor. Because the effective area that the cross covers was a fraction of the total area needed for an effective calibration, extra steps were taken to cover all four corners for each camera lens. This is done in order to compute any lens distortion that may affect computation of the outer perimeters. The ARAMIS system was able to solve approximately 52 square feet of area on the expandable structure.

The system uses a control unit for synchronizing the cameras. This control unit is capable of accepting several analog and digital inputs. One input recorded during the test was from the pressure sensor gage located on the hatch of the expandable structure. The 28 feet diameter expandable structure was filled with air and pressurized at 0.05 psi/min to a max pressure of 5.22 psig.

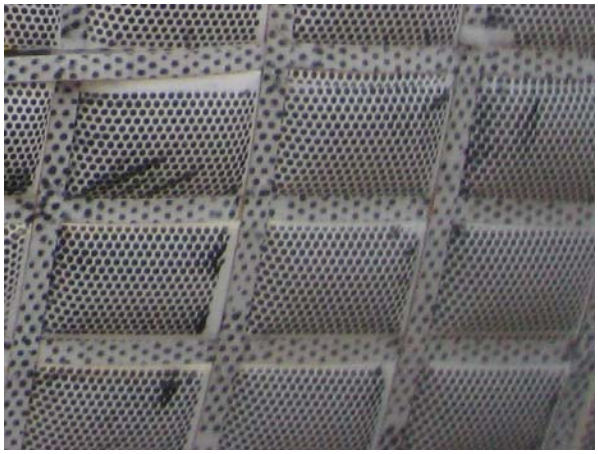

Figure 2. Phase II article with Painted "Dot" Pattern to Support Photogrammetric Analysis (close-up)

Figure 3. Phase II article with Painted "Dot" Pattern and Photogrammetry Camera System

IV. Phase II Test Objectives

The objectives of the Pressurization Tests are to validate assumptions related to (1) integration of a hatch structure into inflatable modules, and (2) correlate analytical predictions of strap loading with measured strain/load utilizing strain gauged and calibrated clevises and photogrammetric strain measurements.

V. Phase II Pre-test Assumptions

(1) At low pressure, scatter in strain gage measurements is expected. However, first order trends will be present. Low pressure strain gage measurements should provide insight into future placement and the capabilities of the strain gages.
(2) Strain measurement as measured by the photogrammetry cameras is expected to provide good data locally and globally.
(3) Analytical predictions are expected to correlate better for the Phase II article better than for the Phase I article due to the additional friction inherent with the woven design.

VI. Overall Design

The Phase II test article consists of a load bearing restraint layer, a bladder or gas barrier, and a structural metallic core. The test article restraint layer consists of one inch wide Kevlar webbing that is fabricated in cargo net pattern (Figure 1). The test article is 28-feet in diameter and 12.3 feet in height and weighs approximately 11,000 lbs when

assembled. The bladder and restraint layer are assembled to a central core structure, which is 12-ft diameter and 12-ft high, to form a full scale inflatable torus. Underneath the structural restraint layer is the bladder or gas barrier. For this test the bladder was required to maintain pressure for testing only and was not representative of a flight design. The bladder and structural restraint layer attach to the structural core of the module at steel bulkheads at each end. The longitudinal members of the structural restraint layer are attached to the bulkheads using a series of clevises that are bolted to the bulkheads. A 40-inch diameter hatch with 49-inch structural frame is integrated into the belly of the fabric. Clevises are also mounted to the structural hatch/frame in the longitudinal and hoop directions and interface with the structural restraint layer. Strain gages are placed on the clevises that can measure change in load when the structural restraint is inflated.

VII. Instrumentation

Phase II article has 7 strain gages that are attached to the roller/clevis assemblies which attach the strap restraints to the hatch/frame. The gages are arranged as shown below in Figure 4 with 4 gages mounted on clevises that interface with cylindrical hoop straps. Three gages are mounted on clevises interfacing with longitudinal straps. After installation of each strain gage, calibration was performed to establish the relationship of microstrain to axial strap load.

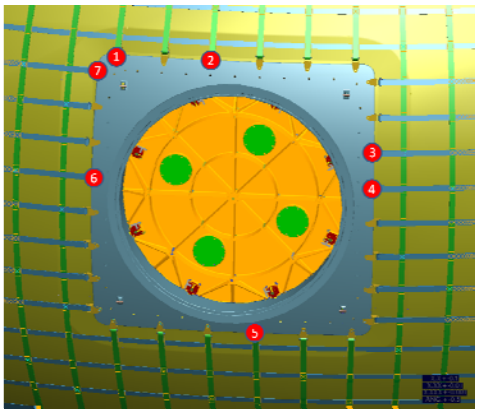

Figure 4. Phase II Hatch/Frame Clevis locations with Strain Gages

VIII. Bench Testing

Bench testing was performed on 1-inch wide Kevlar webbing (rated at 6,000 and 12,500 pound/inch), 1-inch wide Vectran webbing (rated at 12,500 pound/inch), 16,500 pound/inch Vectran cord, and 400 pound/inch Vectran fabric. Three tension pulls were made for each material type. For the webbings extensometers were placed on the test samples 4 inches apart. All materials were painted in the test region with white paint and then black paint in a spackle pattern to support strain measurement using photogrammetry. For Kevlar and Vectran webbing, photogrammetric strain measurement was compared with deflections measured by the extensometers. Photogrammetric strain measurements were taken at the left, center, and right portions along the width of the strap to see how measurements varied. For the Vectran cord and Vectran fabric photogrammetric strain measurement was compared with crosshead deflection.

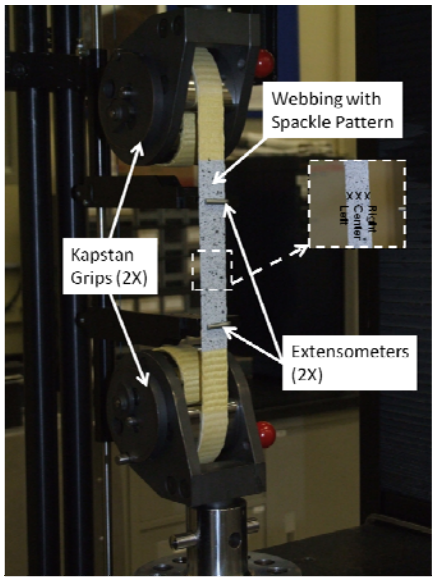

Figure 5. Webbing Set-up for Testing

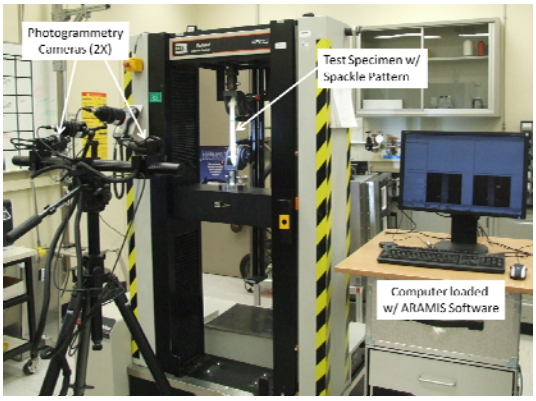

Figure 6. Photogrammetry System Set-up with ARAMIS Program

IX. Results of Bench Testing

The left, center, and right portions along the width of the strap showed a slight difference in strain measurements. Even though these differences are very minimal it is good to note. There were 2-3 runs for each type of webbing, cord, and fabric. For this paper, only the webbing data from the Phase II pressurization test is presented. When comparing the 3 different runs for the webbing, the photogrammetric strain measurements were always less that that measured by the extensometer (Fig. 7). There was a minimal difference between each of the runs which could have resulted from human errors such as differences in test set-up and alignment. From the photogrammetric bench test, strain versus load curves are established and a least squares curve and equation is generated (Fig. 8). These curves are generated from average values generated during the multiple tests. These averages are converted into one final average and equation, so during pressurization testing the strain measured utilizing photogrammetry can be converted to load (Fig. 9).

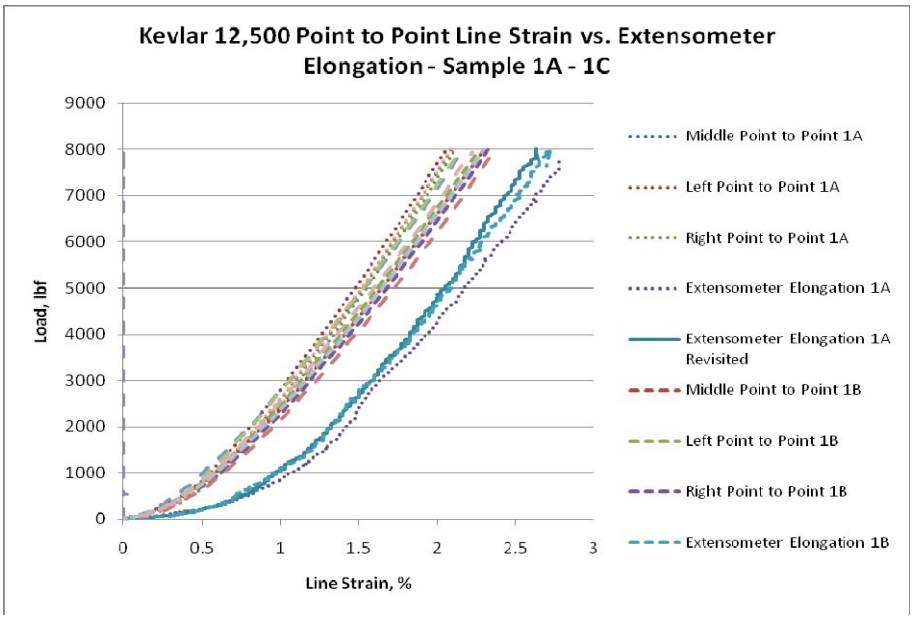

Figure 7. Left, Center, and Right Photogrammetric and Extensometer Strain Measurement versus Load for 12,500 lb/in Kevlar Webbing

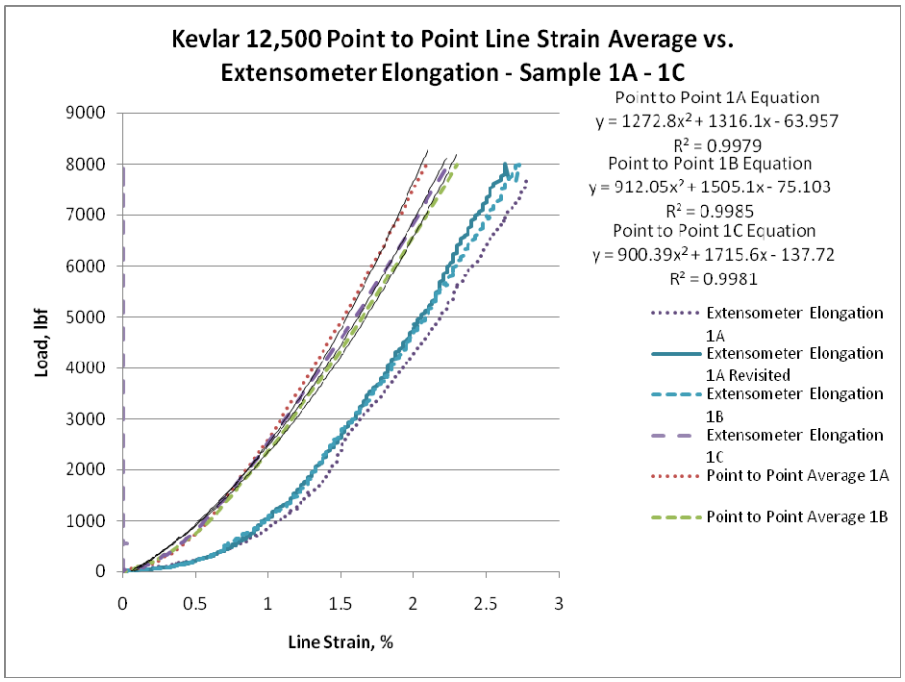

Figure 8. Photogrammetric and Extensometer Strain Measurement versus Load for 12,500 lb/in Kevlar Webbing

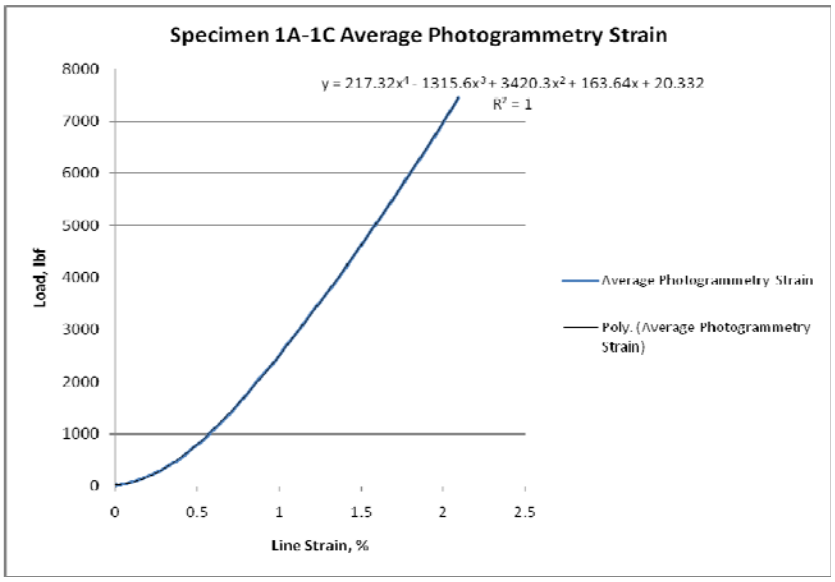

Figure 9. Left, Center, and Right Photogrammetric Average for Three Runs

X. Phase II Test

The test was performed at the Energy Systems Test Area (ESTA) within Johnson Space Center. At first the Phase II article was checked for correct positioning of restraint layer and bladder components at 0.25 psig before continuation. The article was inflated from 0.25-5.22 psig, while strain gage and photogrammetric measurements were being recorded.

XI. Analysis of Phase II Test Data

A. Strain Gage Data Reduction

Load versus strain calibration curves were generated for the seven (7) strain gauged clevises. These curves were utilized to determine load from measured strain during Phase II pressurization testing. Strain gage measurements were obtained from ESTA's computer systems. The longitudinal strain gage data was divided by two, since there was overlapping of Kevlar straps in the longitudinal direction. The hoop strain gage data was left as is, because only one Kevlar strap runs around the entire hoop direction.

B. Photogrammetric Data Reduction

Photogrammetric strain measurements had to go through a process before it can be compared to strain gage and analytical values. Below is an example of the analytical photogrammetric process that was taken at location 1 (refer to Figure 4).

The raw data received from photogrammetry was in pressure (psig) and line strain (%). The first step is to plot a pressure vs. line strain curve. The raw data is displayed below in red (Fig. 10).

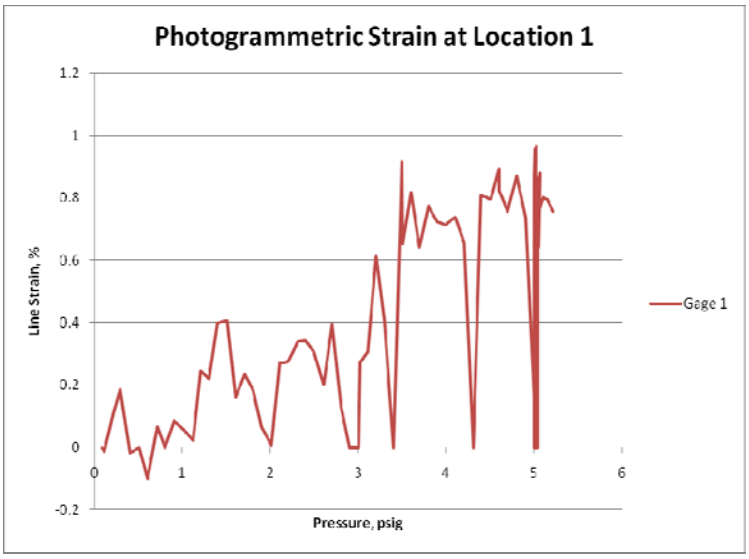

Figure 10. Photogrammetric Raw Data near Gage 1

There is a line strain percentage corresponding to every 0.1 psig increase in pressure. The graph shows a 0% line strain where there are missing data points. There were missing points due to sun over-exposure on the camera lens. The inconsistent spiking in the graph is due to the fact that the field of view was too large and the straps were too small. Although there are erroneous data points, a trend can be concluded from the graph. In order to get the equation of the trend line, the 0% line strain points representing missing data were eliminated from consideration. The remaining points are shown below in blue with its best fit curve and corresponding equation (Fig. 11).

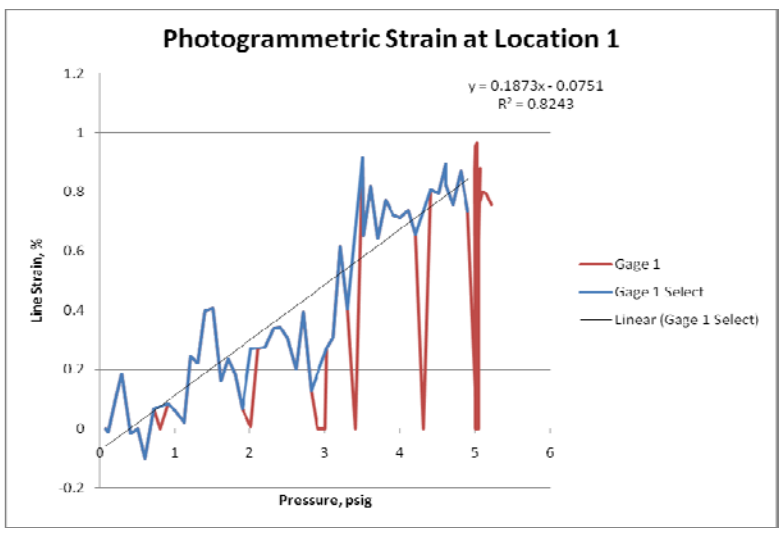

Figure 11. Selected Data Points from Photogrammetric Raw Data near Gage 1

In the equation, for every pressure value we plugged into "x" we got a corresponding line strain percent value "y". This was done to make the graph look smoother and to get rid of the erroneous values that skew the graph. The next step was to normalize this smooth curve if necessary. Normalization was necessary only when slack was noticed. For location 1 there was no slack noticed, but below you can see the slack in the beginning for location 3 and we normalized it by shifting the curve down until the first data point starts at 0 (Fig. 12).

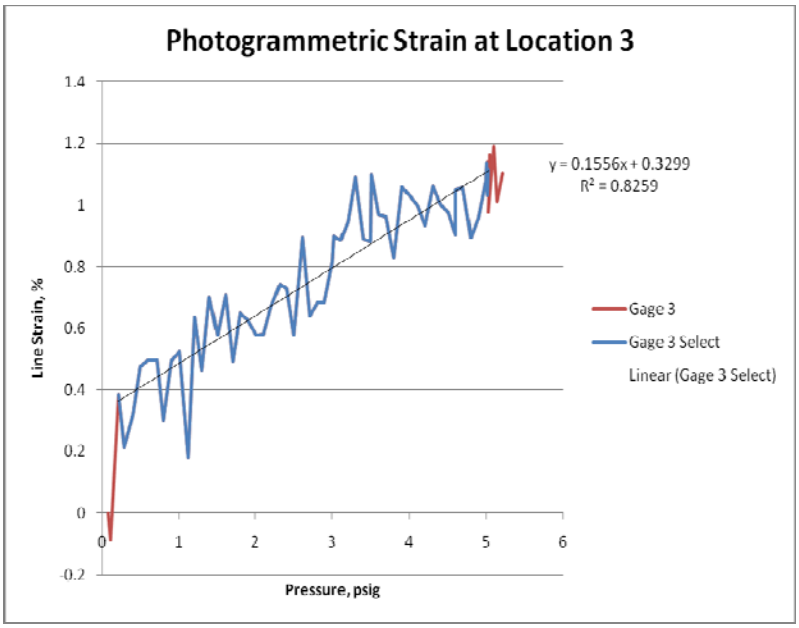

Figure 12. Slack Present at Gage 3 Location

The way we moved this curve down was to subtract the line strain percent by the y-intercept, which was generated by the best fit equation. This puts us at a point in the process where we have a smooth pressure vs. line strain percent curve that has been normalized if necessary (Fig. 13).

Figure 13. Smooth Pressure vs. Line Strain Curve for Gage 1

Now we need to convert from pressure vs. line strain percent to pressure vs. load. From the bench test of Kevlar 12,500 lb/in strap, we generated a photogrammetry equation which gives us a load value "y" for every line strain percent value that is plugged into "x" (Fig. 9). From this equation we converted all the line strain percent values to load. Finally, we can create a graph of pressure vs. load, which is what we want to analyze (Fig. 14).

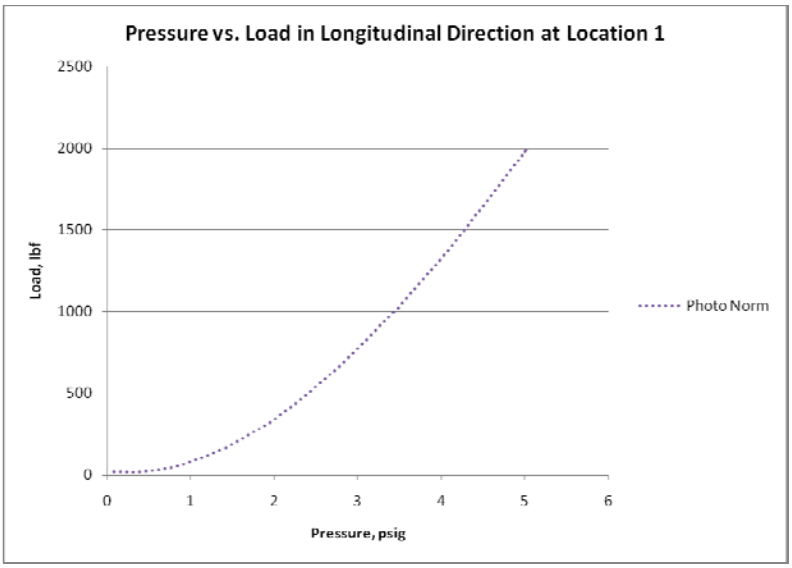

Figure 14. Pressure vs. Load Curve for Gage 1

The comparison of analytical load, gage strain data, and photogrammetric data for location 1 shows similarity in all three curves (Fig. 15). However, most of the locations did not show this. The analytical and strain gage curves seemed to go hand in hand, but the photogrammetric curve was always over predicting load (Fig. 16).

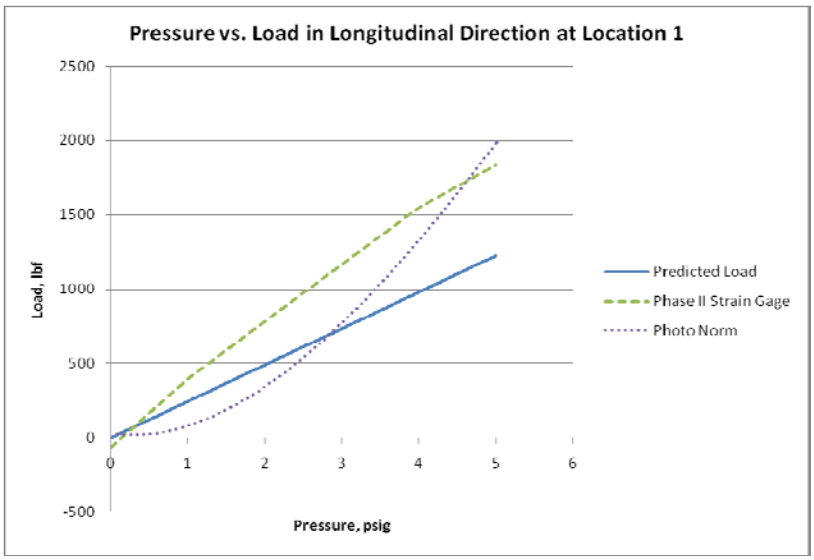

Figure 15. Analytical, Strain Gage, and Photogrammetric Curve Comparison at Location 1

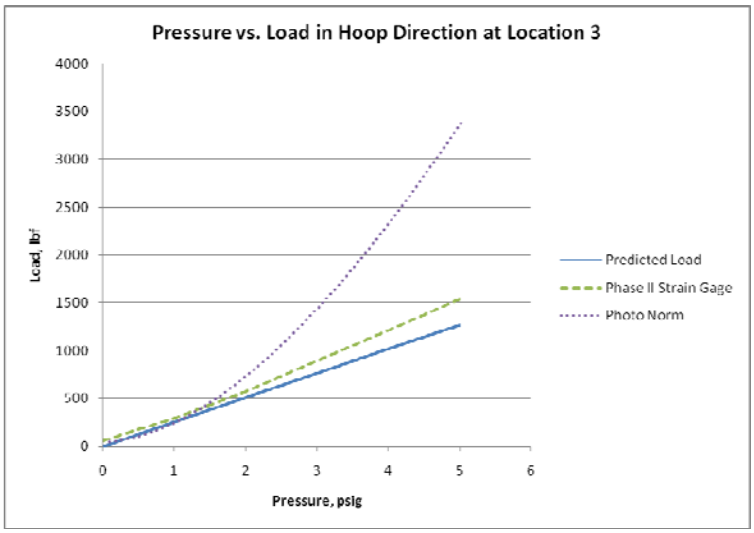

Figure 16. Analytical, Strain Gage, and Photogrammetric Curve Comparison at Location 3

XII. Results of Phase II Data Analysis

The analytical load, strain gage load, and photogrammetric load were recorded at the highest pressure (Table 1).

Phase II Load at 5.22 PSIG				
Location	**Analytical Load**	**Strain Gage Load**	**Photogrammetric Load**	**Photogrammetry Percent Error**
Hoop	**lbf**	**lbf**	**lbf**	**%**
3	1271.2485	1537.8	3389.65	166.6394493
4	1271.2485	1728.5	2645.33	108.0891344
6	1271.2485	1152.635	2905.168	128.5287259
7	1271.2485	1116.605	3811.38	199.8139231
Longitudinal				
1	1224.4	1837.1	1999.248	63.28389415
2	1224.4	1386.05	2746.73	124.3327344
5	1217.1	1492.875	2732.1	124.476214

Table 1. Recorded Analytical, Strain Gage, and Photogrammetric Load at 5.22 PSIG

XIII. Conclusion/Future Work

The behavior of a cargo net construction is currently under study. During Phase II pressurization testing there was good correlation between strain gages mounted on clevises interfacing with the structural webbings and analytical predictions. In most cases, the photogrammetric data over predicted analytical predictions. The possible reasons believed for this are: sun over exposure on camera, wrong field of view, and/or wrong pattern colored on article. The photogrammetry process used is currently being checked for its validity and redundant but dissimilar avenues are being discussed for the next pressurization test. This large torus shaped module will undergo 9 psig pressurization testing and damage tolerance testing in the summer of 2011 at White Sands Test Facility (WSTF). During Damage Tolerance Testing (DTT) one of the straps will be cut and the data obtained will be correlated with analytical predictions created with a dynamic model using LSDYNA. Lessons learned from the Phase II low pressurization test will be incorporated into the 9 psig Damage Tolerance Test.

XIV. Acknowledgments

Author Anil Mohammed would like to thank Inflatable Structures Project Manager Gerard Valle for providing background knowledge and history of inflatable modules. Author would also like to thank John Edgecombe and Molly Selig for providing technical assistance. Anil Mohammed would lastly like to thank Ovidio Oliveras and ESTA's technicians for providing data necessary for analysis.

XV. References

D.M. Revilock, J.C. Thesken, T.E. Schmidt, B.S. Forsythe, "*3D Digital Image Correlation of a Composite Overwrapped Pressure vessel During hydrostatic Pressure Tests*", 2007 SEM Annual Conference and Exposition on Experimental and Applied Mechanics.

J.E. Edgecombe, H. M. de la Fuente, and G.D. Valle, "Damage Tolerance Testing of a NASA TransHab Derivative Woven Inflatable Module", 2009 AIAA/ASME/ASCE/AHS/ASC Structures, Structural Dynamics, and Materials Conference, AIAA-2009-2167.

J. Hinkle, A. Dixit, J.K. Lin, K. Whitley, J. Watson, G. Valle, "Design Development and Testing for an Expandable Lunar Habitat", Space 2008 Conference and Exposition.